Multi-machine scaling of the main SOL parallel heat flux width in tokamak limiter plasmas

2016 Plasma Phys. Control. Fusion 58 074005

(http://iopscience.iop.org/0741-3335/58/7/074005)

OPEN ACCESS
IOP Publishing
Plasma Physics and Controlled Fusion
Plasma Phys. Control. Fusion **58** (2016) 074005 (11pp)
doi:10.1088/0741-3335/58/7/074005

Multi-machine scaling of the main SOL parallel heat flux width in tokamak limiter plasmas

J Horacek[1], R A Pitts[2], J Adamek[1], G Arnoux[3], J-G Bak[4], S Brezinsek[5], M Dimitrova[1], R J Goldston[6], J P Gunn[7], J Havlicek[1,8], S-H Hong[4], F Janky[1,8], B LaBombard[9], S Marsen[10], G Maddaluno[11], L Nie[12], V Pericoli[11], Tsv Popov[13], R Panek[1], D Rudakov[14], J Seidl[1], D S Seo[4], M Shimada[15], C Silva[16], P C Stangeby[17], B Viola[11], P Vondracek[1,8], H Wang[18], G S Xu[18], Y Xu[5] and JET Contributors[19]

[1] Institute of Plasma Physics ASCR, Za Slovankou 3, Prague, 18000, Czech Republic
[2] ITER Organization, CS 90 046, 13067 St. Paul Lez Durance Cedex, France
[3] EUROfusion Consortium, JET, Culham Science Centre, Abingdon, OX14 3DB, UK
[4] National Fusion Research Institute, Gwahangno 113, Yuseong-Gu, Daejeon, 305-333, Korea
[5] Juelich Forschungszentrum, Jülich, Germany
[6] Princeton, Plasma Physics Laboratory, Princeton, NJ 08543, USA
[7] CEA, IRFM, F-13108 Saint-Paul-lez-Durance, France
[8] Faculty of Mathematics and Physics, Charles University, Prague, Czech Republic
[9] Massachusetts Institute of Technology, Plasma Science and Fusion Center, 175 Albany St., Cambridge, MA 02139, USA
[10] Max-PLanck-Institut fur Plasmaphysik, Teilinstitut Greifswald, D-17491 Greifswald, Germany
[11] ENEA-UT Fusione, Centro Ricerche Frascati, Rome, Italy
[12] Southwestern Institute of Physics, Chengdu, People's Republic of China
[13] Faculty of Physics, St. Kliment Ohridski University of Sofia, J. Bourchier Blvd., 1164 Sofia, Bulgaria
[14] University of California, San Diego, Center for Energy Research, Fusion Division, 9500 Gilman Dr, Mail code 0417, EBU II, Rm 468, La Jolla, CA 92093-0417, USA
[15] Japan Atomic Energy Agency, 2–166 Oaza-Obuchi-Aza-Omotedate, Rokkasho-mura, Kamikita-gun, Aomori 039-3212, Japan
[16] Instituto de Plasmas e Fusao Nuclear, Institute Superior Tecnico, Universidade Lisboa, Lisbon, Portugal
[17] University of Toronto, Institute for Aerospace Studies, Toronto, M3H 5T6, Canada
[18] Institute of Plasma Physics, Chinese Academy of Sciences, Hefei 230031, People's Republic of China

E-mail: horacek@ipp.cas.cz

Received 30 November 2015, revised 14 March 2016
Accepted for publication 21 March 2016
Published 31 May 2016

Abstract

As in many of today's tokamaks, plasma start-up in ITER will be performed in limiter configuration on either the inner or outer midplane first wall (FW). The massive, beryllium armored ITER FW panels are toroidally shaped to protect panel-to-panel misalignments, increasing the deposited power flux density compared with a purely cylindrical surface. The chosen shaping should thus be optimized for a given radial profile of parallel heat flux, $q_{||}$ in the scrape-off layer (SOL) to ensure optimal power spreading. For plasmas limited on the outer wall in tokamaks, this profile is commonly observed to decay exponentially as $q_{||} = q_0 \exp(-r/\lambda_q^{\mathrm{omp}})$, or, for inner wall limiter plasmas with the double exponential decay comprising a sharp near-SOL feature and a broader main SOL width, λ_q^{omp}. The

[19] See the appendix Romanelli F *et al* 2014 *Proc. of the 25th IAEA FEC (St. Petersburg, Russia)*

initial choice of $\lambda_q^{\rm omp}$, which is critical in ensuring that current ramp-up or down will be possible as planned in the ITER scenario design, was made on the basis of an extremely restricted L-mode divertor dataset, using infra-red thermography measurements on the outer divertor target to extrapolate to a heat flux width at the main plasma midplane. This unsatisfactory situation has now been significantly improved by a dedicated multi-machine ohmic and L-mode limiter plasma study, conducted under the auspices of the International Tokamak Physics Activity, involving 11 tokamaks covering a wide parameter range with $R = 0.4$–2.8 m, $B_0 = 1.2$–7.5 T, $I_{\rm p} = 9$–2500 kA. Measurements of $\lambda_q^{\rm omp}$ in the database are made exclusively on all devices using a variety of fast reciprocating Langmuir probes entering the plasma at a variety of poloidal locations, but with the majority being on the low field side. Statistical analysis of the database reveals nine reasonable engineering and dimensionless scalings. All yield, however, similar predicted values of $\lambda_q^{\rm omp}$ mapped to the outside midplane. The engineering scaling with the highest statistical significance, $\lambda_q^{\rm omp} = 10(P_{\rm tot}/V\ ({\rm W\,m^{-3}}))^{-0.38}(a/R/\kappa)^{1.3}$, dependent on input power density, aspect ratio and elongation, yields $\lambda_q^{\rm omp} = [7, 4, 5]$ cm for $I_{\rm p} = [2.5, 5.0, 7.5]$ MA, the three reference limiter plasma currents specified in the ITER heat and nuclear load specifications. Mapped to the inboard midplane, the worst case (7.5 MA) corresponds to $\lambda_q^{\rm imp} \sim 57 \pm 14$ mm, thus consolidating the 50 mm width used to optimize the FW panel toroidal shape.

Keywords: tokamak, ITER, SOL decay length, SOL width, scaling

(Some figures may appear in colour only in the online journal)

1. Introduction

As in many tokamaks, ITER will use the main chamber first wall (FW) as a limiter for a part of the plasma ramp-up and down phases. For a variety of reasons, the high field side (HFS) midplane is presently favoured for ramp-up, with baseline scenarios to the nominal 15 MA of plasma current passing through an initial circular, then elongated limiter phase up to around 3.5 MA before the transition to a diverted configuration some 10–15 s after plasma initiation [1]—see figure 1. Ramp-down is expected to occur preferentially on the outer wall, with limiter contact likely only at extremely low plasma current.

The ITER FW consists of 440 blanket modules, each comprising a massive steel shield block protected by a beryllium armoured panel. The latter is constituted of poloidal arrays of toroidally extended, water cooled fingers made up of Be flat tiles bonded to a copper chromium zirconium heat sink, itself bonded to a steel structure bearing the water cooling channels [2]—see figures 2(a) and (b). To account for the high heat fluxes expected during limiter operation, the inner and outer midplane (omp) panels are of a hypervapotron design, permitting power flux densities of up to 4.7 MW m^{-2} in steady state. The fingers are shaped toroidally to magnetically shadow the central recessed remote handling slot and to hide leading edges arising from possible misalignments between neighbouring blanket modules [3].

The FW panel toroidal shaping has been chosen on the basis of analytic studies supported by numerical simulations to optimize power loading for a given scrape-off layer (SOL) parallel heat flux profile [4]. Based on a large number of observations on tokamaks, this profile was originally chosen as a single exponential decrease with radius from the last closed flux surface (LCFS) $q_{||} = q_0 \exp(-r_{\rm mid}^{\rm LCFS}/\lambda_q^{\rm omp})$, with $\lambda_q^{\rm omp}$ the characteristic SOL heat flux width and $y = r_{\rm mid}^{\rm LCFS} = r - r_{\rm LCFS}$ the radial distance from the LCFS. This radial profile is traditionally specified at the omp. As shown in [4], if the SOL heat flux has this form, a logarithmic toroidal shape given by

$$y = -\lambda_q^{\rm omp} \cdot \ln\left(1 - \frac{C \cdot x}{\lambda_q^{\rm omp}}\right), \qquad (1)$$

theoretically provides for a constant deposited heat flux across the limiter surface (see figure 2(c)). Recently, it has become clear that the limiter SOL heat flux is more complex and can in fact be described in a large number of devices by a double exponential, characterized by a very narrow near SOL feature and a broader main SOL fall-off [1]. The ITER inner wall FW panel shaping has recently been modified to account for these new observations [1].

Central to the shape design is the value of $\lambda_q^{\rm omp}$, which is not known for ITER and which must thus be chosen either from a scaling or physics-based appproach. It must, moreover, be a fixed value with sufficient margin to encompass the range of plasma currents and magnetic configurations envisaged for limiter plasmas on ITER (see below). In fact, two separate values of the heat flux width are required, one each for the narrow and broad SOL features. The choice of the narrow feature is discussed in [1] and references therein, and the present paper concentrates on the main SOL, broader portion of the profile. We will henceforth refer to the characteristic width associated with this part of the profile as $\lambda_q^{\rm omp}$ to emphasize its specification at the omp.

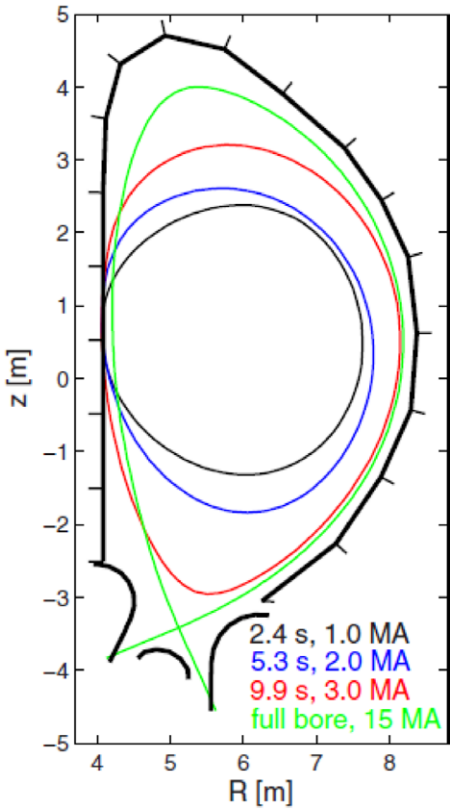

Figure 1. Plasma current ramp-up sequence of magnetic configuration of ITER start-up scenario (from [1]).

In the absence of a database for limiter plasmas, the original choice of $\lambda_q^{\rm omp}$ for the ITER FW panel shaping was based on scaling from a set of infra-red measurements on the divertor targets of L-mode discharges in the JT-60U, JET and ASDEX-Upgrade tokamaks [5, 6]. Unfortunately, this scaling was later shown to be inconsistent with an extensive set of SOL heat flux measurements in circular limiter plasmas on the Tore Supra tokamak [7]. As divertor discharges can, in principle, have different decay lengths (thus not useful for design of ITER limiter), these observations stimulated an extensive, multi-machine study of the main SOL heat flux width in inner wall limiter discharges requested by the ITER Organization (IO) and conducted under the auspices of the International Tokamak Physics Activity (ITPA) Topical Group on Divertor and SOL physics. This paper presents the results of this database activity, develops a variety of possible scalings from the data and provides recommendations for the values of $\lambda_q^{\rm omp}$ to be used in the ITER FW shaping design. It concludes that the values originally adopted by the IO for the high and low field side start-up/ramp-down panels are appropriate.

Based on simple power balance, assuming the sheath-limited parallel heat flux physics, $\lambda_q^{\rm omp}$ should be approximated by the power entering the SOL as $\lambda_q \sim P_{\rm SOL}B_0/(B_{\rm pol}2\pi R_0 n_{\rm e}T_{\rm e}^{3/2})$. The emphasis here is, however, on the use of engineering parameter based scalings which are most appropriate for extrapolation to ITER, where the midplane plasma parameters in limiter discharges are not known. This does not preclude a more physics based approach and a companion paper in this special issue [8] describes a theoretical framework based on quasi-linear transport theory which agrees very favourably with a subset of the ITPA database presented in this paper.

2. Multi-device experiment and methodology

2.1. Participating tokamaks

A total of eleven devices have contributed measurements to the new ITPA limiter heat flux width database. In the majority of cases (exceptions are data from the CASTOR and Tore-Supra tokamaks), specific new experiments have been performed at the request of ITPA and, with the exception of the CASTOR tokamak, all have concentrated on inner wall limiter discharges, reflecting the emphasis on this configuration for the important ramp-up phase of ITER plasmas. Moreover, in most cases, the location of diagnostics on the outboard side of the machine, together with the often limited experimental time resource, means that focus on a single type of equilibrium (which can be adequately probed) provides the best chance for a well populated database.

Figure 3 compiles the poloidal cross-sections of the participating tokamak devices, including the typical magnetic equilibria employed in the studies. Of the 11 machines, TEXTOR, Tore-Supra, CASTOR and FTU are pure limiter devices. All others are divertor tokamaks, typically using a brief limiter phase, usually on inner wall plasma-facing components (PFC), before transition to a diverted configuration. In these cases, dedicated limited only discharges have been performed so that the majority of measurements are taken in stationary limiter plasmas. A key feature of these divertor tokamak limiter plasma studies is that they are generally conducted in non-circular equilibria, since such shapes are typically easier to achieve over a reasonable range of plasma parameters.

A wide range of machine parameters is encompassed by the database (table 1), with plasma current, $I_{\rm p} = 9$ kA $\rightarrow 2.5$ MA, toroidal magnetic field, $B_0 = 1.15$–7.5 T, line average plasma density $\overline{n}_{\rm e} = 0.5 \rightarrow 25 \times 10^{19}$ m^{-3} and safety factor ($q_{\rm omp}$ or q_{95} for non-circular plasmas) $= 2.2 \rightarrow 13$. The database also spans a large range of physical dimension (major radius $R_0 = 0.4 \rightarrow 2.8$ m) from the smallest machine, CASTOR with plasma volume $V = 0.06$ m^3 to the largest, JET, with $V = 70$ m^3. The majority of measurements are made in ohmic plasmas, but some data points have been obtained with additional heating. On ITER, some low levels of electron cyclotron resonance heating (ECRH) are envisaged during plasma ramp-up, but densities will generally be below the limits required for neutral beam injection (NBI) shinethrough.

2.2. Measurement technique

Scrape-off layer heat flux profiles have been obtained exclusively with a variety of reciprocating Langmuir probes (RCP), inserted into the edge plasma at different poloidal locations, but with the majority entering on the outboard midplane. Figure 3 illustrates the RCP entry points superimposed on the machine poloidal cross-sections along with typical examples of the magnetic equilibrium reconstructions used in the

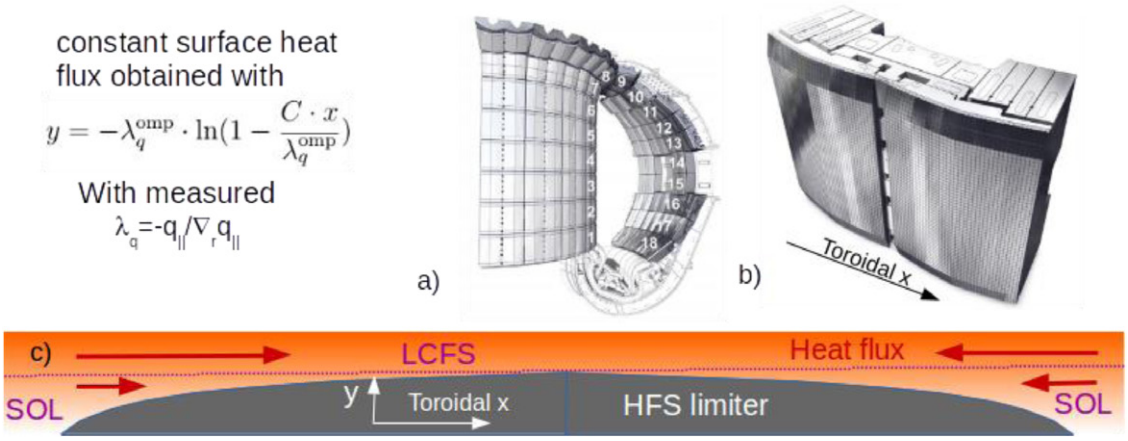

Figure 2. (a) 3D drawing of the ITER inner wall consisting of 440 panels (enlarged in (b)) [1]. (c) Schematic limiter contour optimized for toroidally constant surface power everywhere for a SOL plasma characterised by exponential decay length λ_q^{omp}. The constant C is determined by the required setback at the toroidal extremities, itself determined by the panel to panel radial misalignment the shaping must protect.

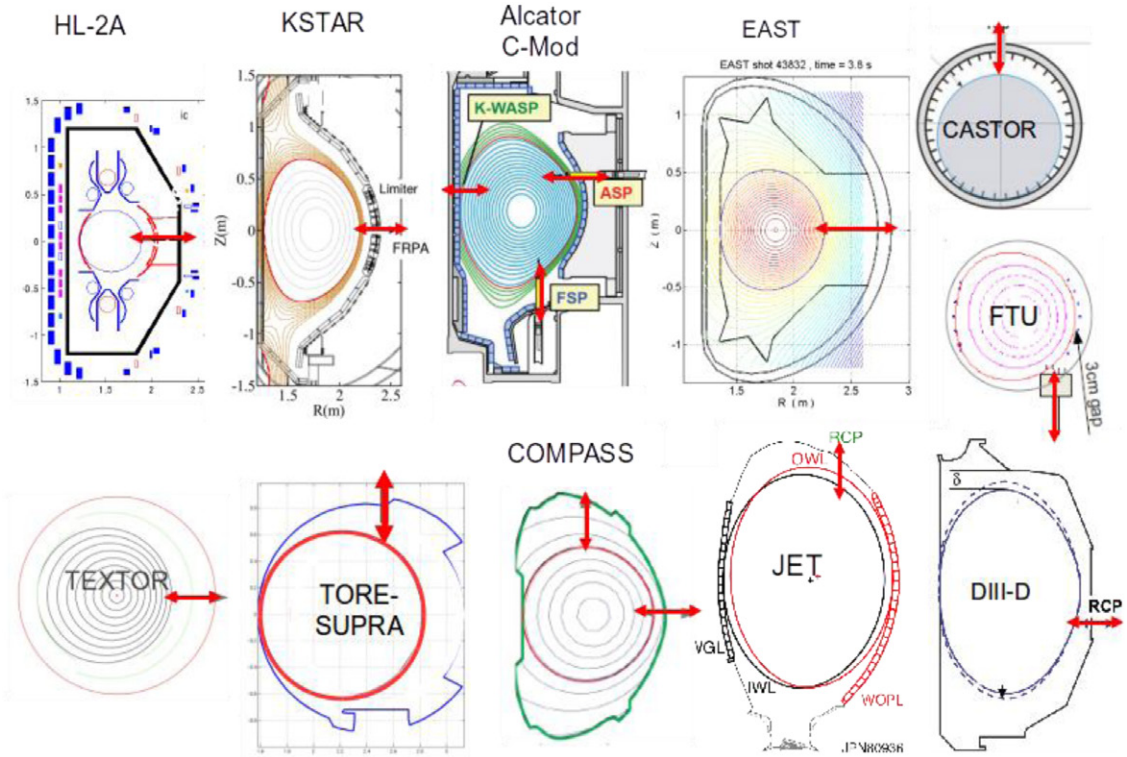

Figure 3. Plasma shapes (not to scale) of all the tokamaks providing input data. The reciprocating Langmuir probe positions are marked by red arrows.

experiments. Table 1 lists the poloidal angle of entry relative to the outboard midplane defined as $\theta = 0°$, together with a description of the probe technique used on each device.

Figure 4 gives an example of the profiles and their fits. To obtain λ_q^{omp}, the probes are used to measure the SOL radial profiles of plasma electron temperature, T_e and ion particle flux density, j_{sat}. These profiles are then mapped (if necessary) around to the outside midplane and combined to obtain $q_{||}$ as a function r_{mid}^{LCFS}. Assuming the SOL plasma to be in the sheath-limited regime [9], and given the usual exponential nature of the profile in the main SOL, λ_q^{omp} can be obtained either by fitting $q_{||}$ directly using $q_{||} = \gamma j_{sat} T_e$, with γ the sheath heat transmission coefficient (assumed constant), or by combining the characteristic widths derived separately from the T_e and j_{sat} profiles and applying the relation $\lambda_q^{omp} = [\lambda_{T_e}^{-1} + \lambda_{j_{sat}}^{-1}]^{-1}$, valid for the simple SOL [9]. The advantage of the latter approach is that j_{sat} profiles can typically be measured with high time resolution, transferring to high spatial resolution for a probe which reciprocates rapidly in and out of the SOL plasma. Both approaches (fitting profiles of $q_{||}$ and combining separate fits from T_e and j_{sat} profiles) have been tested on the JET data (see figure 5), including a 'human factor' arising from different individuals processing data from identical discharges. The second approach seems to yield data with less scatter.

Table 1. Overview of principal parameters of the tokamak limiter plasmas used to constitute the multi-machine database. The projected ITER values, where known, are shown for comparison. Figure 5 provides further information on the parameter variation in the database. The poloidal angle corresponds to the poloidal location at which the Langmuir probes used to make the measurements, with 0 corresponding to the outboard midplane. BPP = ball pen probe; RFA = retarding field analyser. NBI = neutral beam injection heating; ECH = electron cyclotron heating.

	R_0 (m)	a (m)	I_p (kA)	B_0 (T)	No. data points	Additional heating	Fuel species	Measurement of T_e	Poloidal angle
ITER	6.0	2.0	3500–7500	5.3	3	ECH	H, D, He, T	—	—
JET	2.8	0.98	1500, 2500	2.8	33	0	D	Swept Langmuir	90°
Tore Supra	2.2	0.65	500–1200	2.6–4.1	121	0	D	Tunnel + RFA	90°
DIII-D	1.7	0.6	600–1200	1.9	23	NBI	D	Harmonic technique	−25°
C-Mod	0.68	0.22	400–1100	4–7	19	0	D	Scanning mirror	30°
KSTAR	1.78	0.47	400	2.0	1	NBI	D	Triple probe	0°
TEXTOR	1.73	0.46	±200–400	±1.3–2.6	55	NBI	D	Triple probe	0°
EAST	1.85	0.46	300	1.96	2	0	D	Triple probe	0°
HL-2A	1.67	0.36	100–220	1.36	39	ECH + NBI	D	Triple probe	0°
FTU	0.94	0.28	250–500	2.7–7.5	3 × 9	0	D	Swept Langmuir	−60°
COMPASS	0.55	0.2	80–180	1.15	91	0	H, D	BPP, swept Langmuir	0°, 90°
CASTOR	0.4	0.08	9	1.3	3	0	H	Swept Langmuir	90°

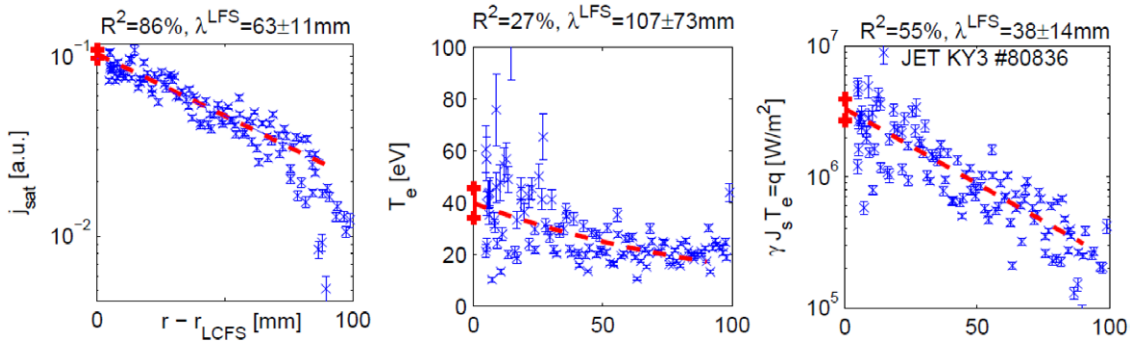

Figure 4. Example of radial profile fitting of ion saturation current j_{sat}, T_e and $q_{\parallel} \sim j_{sat}T_e$ from the JET vertical reciprocating probe. Error bars resulting from the fits are taken for further processing in figures 5 and 6. Fit extrapolation up to LCFS is required for calculation of omp LCFS plasma parameters ν^{omp}_{gbs}, ρ^*, β_{omp}. Even though steep gradients have been observed in the near SOL region [1, 20] at the high field side (HFS), in our database it is never present outside the LCFS, making simple exponential extrapolation credible. This often leads to large error bars (shown by the vertical bars at $r - r_{LCFS} = 0$, depending especially on how close to LCFS the probe could penetrate) in these variables, which is also taken into account in further processing.

2.3. Possible systematic errors

In some cases, fast T_e data is also available, for example using the mirror probe technique on C-Mod [10], the harmonic sweeping method on DIII-D [11], a triple probe on EAST [12], Langmuir-ball-pen (BPP) on COMPASS [13], or the tunnel probe on Tore-Supra [14]. The disadvantage is that using this higher resolution data requires more than one probe tip and so the measurements are not made at precisely the same location in the SOL plasma. Since $\lambda_{T_e} \gg \lambda_{j_{sat}}$ is almost always found in the measurements used (and is expected on the basis of simple considerations [9]), the resulting value of λ^{omp}_q is only weakly dependent on λ_{T_e}, and is thus relatively independent of the particular T_e-measurement technique. Indeed, on COMPASS both the BPP-LP [13] and standard swept Langmuir probe techniques (cross-checked e.g. in [13, 15]) were used at the low-field side (LFS) location and no systematic difference in the derived λ^{omp}_q was found. With the above points in mind, and given that each device provides processed measurements resulting from the analysis methods in use by any particular group providing data, results from both fitting approaches have been used to constitute the database. The three representative CASTOR datapoints were extracted from publications [16–19].

Where possible (in our case only for COMPASS, TEXTOR and JET data, for which errors from the fit to λ^{omp}_q are available), to capture the relative quality of any given fit assuming an exponential profile, we assign a *statistical relative weight* for each λ^{omp}_q data-point according to

$$\text{weight} = \frac{\lambda^{omp}_q}{\sigma_\lambda} \frac{1}{\sqrt{1-R^2}}, \qquad (2)$$

where σ_λ is error of λ^{omp}_q from the exponential fitting and *the index of determination* R^2 corresponds to the overall fit quality. In the example in figure 4 left, $R^2 = 86\%$, meaning that 86% of the data variation is explained by this fit (assuming the remaining 14% is due to random scatter). The same approach is used for the individual probe IV-characteristic fitting (again, only in the case of COMPASS, TEXTOR and JET), where each T_e, j_{sat} extracted

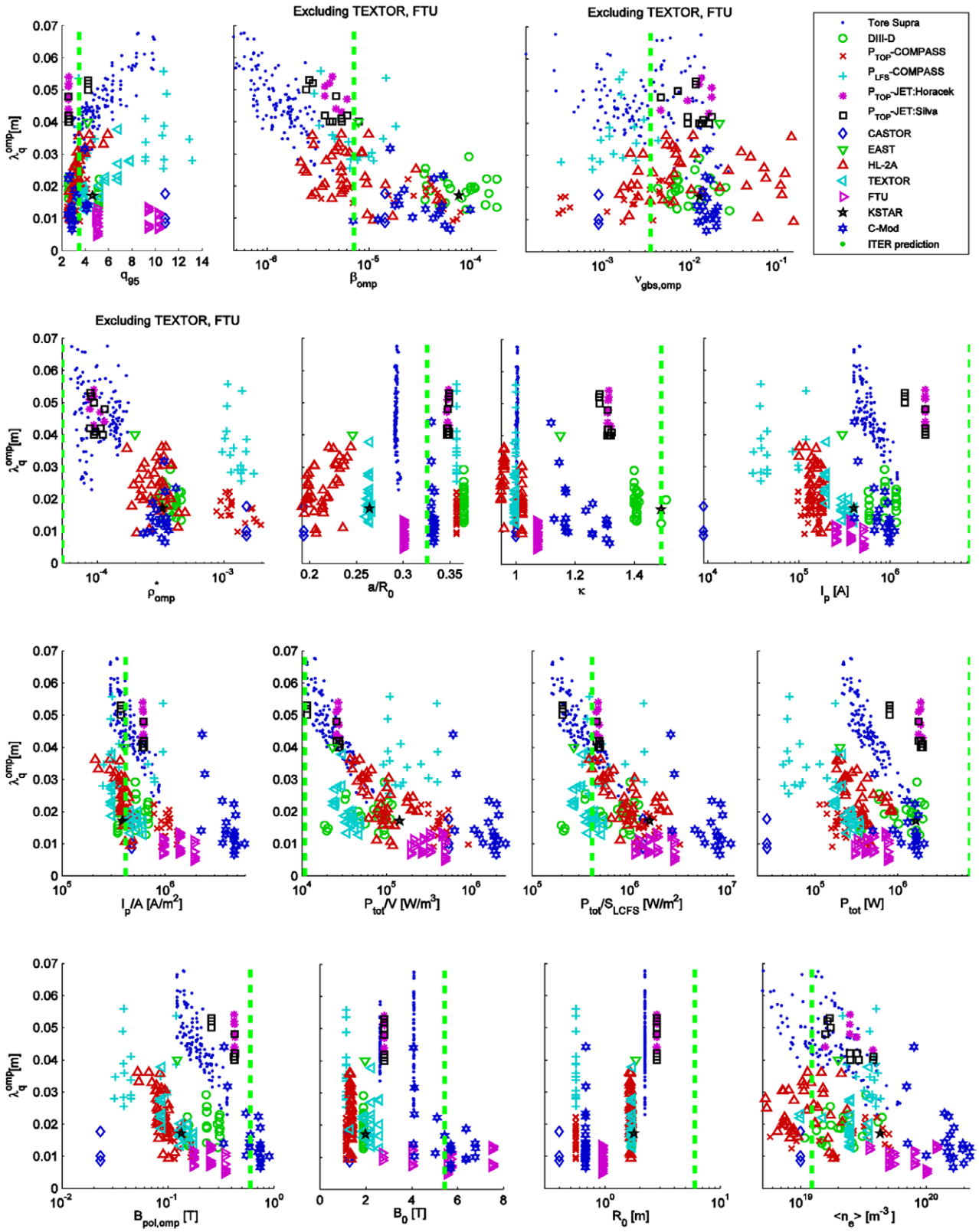

Figure 5. Overview of the full database: $\lambda_q^{\rm omp}$ varying with each of the 15 independent parameters for all 11 tokamaks. The green vertical line corresponds to the 7.5 MA scenario. There is large uncertainty in the values of $\beta_{\rm omp}$, $\rho^*_{\rm omp}$ and $\nu^{\rm omp}_{\rm gbs}$ for ITER. Note that these plasma physics parameters could not be computed for TEXTOR and FTU owing to lack of the required data.[20]

from the fit is associated with an independent error estimate $\sigma_{\rm T}$, σ_j calculated according to formula derived in [21].

We find *a posteriori* that less credible (i.e. lower weight) $\lambda_q^{\rm omp}$ data points usually lie further from derived scalings. The quality of less exponential, noisy or scattered

[20] The full database is available on demand (horacek@ipp.cas.cz).

IV-characteristics (due, for example to the presence of plasma turbulence) is also usually well quantified by the weight$_T = T_e/\sigma_T(1 - R^2)^{-1/2}$ of temperature estimation. For the majority of device data, for which the required input is missing (which prevented the application of equation (2)), equal statistical weighting was assumed for all datapoints, ensuring of course that the total weight of any given device accounts for the number of datapoints contributed.

3. Database overview and choice of scaling parameters

The complete ITPA SOL heat flux database presented here contains 400 probe reciprocations (thus 400 values of λ_q^{omp}) across all devices, with the SOL entry points covering the range $\theta = -60° \rightarrow +90°$ in poloidal angle (table 1). As mentioned in the introductory remarks of section 1, the approach is to scale the data mainly on the basis of engineering parameters only. This is both because plasma parameters for ITER limiter plasmas are not yet known and because there is still no accepted physics basis allowing projection to ITER on the basis of plasma parameters measured on today's devices.

Part of the here-described database has been already used in benchmarking an analytical model [31], which later led to development of GBS simulation described in a companion paper [8] in this special edition. It uses this ITPA database to examine the credibility of a physics based approach founded on quasi-linear turbulent transport theory describing the cross-field heat convection and can claim some success, giving hope that future theoretical progress will provide a solid physics basis for exatrapolation to ITER. The parameters used in [8], normalized plasma pressure $\beta_{omp} = n_e^{omp} T_e^{omp} e/(2\mu_0 B_{omp}^2)$, Larmor radius normalized to the major radius $\rho^*_{omp} = (T_e^{omp} m_i/e)^{1/2} R_0^{-1} B_0^{-1}$ and modified collisionality $\nu_{gbs,omp} = e^2 n_e^{omp} R_0 e \nu_{Spitzer}/(m_i c_s)$ (with $\nu_{Spitzer} = 0.51 \times 10^{-4} \ln(\Lambda) T_e^{-1.5}, \Lambda = 17$, where 'omp' corresponds to the probe locations nearby omp) are neither well-known for ITER nor typically precisely measured in current tokamaks, due mainly to imprecise knowledge of the LCFS position. However, we find in section 4 that these parameters have indeed strong links to the database, as also expected by theory [8]. Perhaps surprisingly, given the large uncertainty in the expected ITER omp plasma temperature and density, the ITER-predicted values of λ_q^{omp} in section 4 using the midplane parameters are also found very similar to those obtained using only engineering parameters. We therefore retain these parameters for consideration in scalings.

The engineering parameters are precisely known: elongation κ, size a, R_0, magnetic field (both B_0 and poloidal field, $B_{pol} = \mu_0 I_p/(2\pi a((1 + \kappa^2)/2)^{1/2})$, I_p, net power crossing the LCFS etc. The strategy is also to try scalings such that ITER lies within the chosen parameter ranges. Thus, for example, scaling variables are chosen as ratios, such as the aspect ratio, a/R_0, the ratio I_p/A with A the plasma cross-sectional area used in place of I_p alone, volumetric power density P_{tot}/V, with P_{tot} the total input heating power (dominated in most cases by the ohmic heating power, P_Ω) or P_{SOL}/S_{LCFS}, with P_{SOL} the power crossing the LCFS ($P_{SOL} = P_{tot} - P_{rad}$, with P_{rad} the power radiated inside the LCFS and S_{LCFS} the surface area of the LCFS).

A further criterion determining the choice of engineering scaling variables is the potential for an impact on the SOL width. An example is the SOL magnetic connection length, $L_c = \pi q_{95} R_0 \propto B_0/I_p$ since this is directly linked to the parallel collisionality and the latter is known to affect SOL perpendicular transport (for example higher collisionality tends to broaden the SOL and this is favoured for longer L_c at fixed SOL density [22]). A related parameter might also be the poloidal angle at which the SOL heat flux profile is measured on each device (see table 1) since SOL turbulence has been shown to be ballooning in character and varies with poloidal location on the LFS [23–25].

The choice of parameters is also determined by the degree to which they can be precisely known for each of the tokamaks contributing to the database. This is the case for almost all the engineering parameters mentioned above with the exception of P_{SOL}, which relies on a good measure of the core radiated power, a quantity not always available to good accuracy on all devices and sometimes simply unavailable. This is in fact the case here, with P_{SOL} values unavailable for 14% of the entries in the database.

Note that the line averaged density, $\bar{n}_e$ though it is often considered as an engineering scaling parameter and is a standard experimental measurement with good accuracy on all tokamaks, is more difficult here since the values to be expected during the ITER ramp-up/down are not known and have only been thus far estimated using transport code simulations without a realistic model of the boundary plasma. We nevertheless include $\bar{n}_e$ as a scaling parameter (or normalized to the Greenwald density limit [26], $n_{e,Gw} = 10^{20} I_p/(\pi a^2 \kappa)$ with I_p in MA), but will in fact find in section 4 that the dependence of λ_q^{omp}on this variable is very weak.

We therefore arrive at a list of engineering parameters to be used in the scaling*:* I_p, I_p/A, R_o, a/R_0, P_{tot}/V, B_0, B_{POL} (evaluated at the omp), q_{omp} (or q_{95} for non-circular equilibria), κ, P_{SOL}/S_{LCFS}, $\bar{n}_e$ and θ (poloidal angle of the SOL heat flux profile measurement). With the exception of R_0 and P_{tot}/V, the ITER values of these parameters all fall within the numerical range of the database (see figure 5). For reference, table 2 compiles numerical values of these parameters for ITER at the three representative values of I_p used to estimate design heat fluxes for the beryllium FW panels in the ITER heat and nuclear load specifications.

The ITER specification for these ramp-up/down scenarios assumes P_{SOL} (MW) $= I_p$ (MA), including ohmic heating and allowing for some additional ECRH heating power. The 7.5 MA value is the maximum specified current at which the inboard and outboard midplane FW panels must be able to sustain steady state limiter plasma operation. In fact, as shown in [1], this equivalence of I_p and P_{SOL} means that the actual value of I_p is unimportant in estimating the parallel heat flux impinging on the limiters which is completely determined by λ_q.

Table 2. Representative values for ITER of the dimensionless (left) and engineering (right) parameters used in scaling the ITPA database for $\lambda_q^{\rm omp}$.

q_{95}	a/R_0	m	$\rho^*_{\rm omp}$	$\beta_{\rm omp}$	κ	$I_{\rm p}$ (MA)	$P_{\rm tot}$ (MW)	$I_{\rm p}/A$ (MA m^{-2})	$\frac{P_{\rm tot}}{V}$ (kW m^{-3})	$\frac{P_{\rm tot}}{S_{\rm LCFS}}$ (MW m^{-2})	$B^{\rm omp}_{\rm pol}$ (T)	B_0 (T)	R_0 (m)	$\overline{n}_{\rm e}$ (10^{18} m^{-3})
9.5	0.33	0.00089	4.2×10^{-05}	1.5×10^{-06}	1.3	2.5	2.5	0.15	4.1	0.15	0.22	5.5	6	4
6	0.34	0.002	4×10^{-05}	2.7×10^{-06}	1.6	5	5	0.24	6.5	0.24	0.37	5.5	6	8
3.5	0.33	0.0035	3.9×10^{-05}	4×10^{-06}	1.5	7.5	7.5	0.41	11	0.41	0.6	5.4	6.1	12

The core density values (at 20% Greenwald limit) are estimates only from transport simulations and are thus indicative. Note that there are large uncertainties in the values of $\beta_{\rm omp}$, $\rho^*_{\rm omp}$ and $\nu^{\rm omp}_{\rm gbs}$.

Table 3. Mutual correlations (%) between logarithms of parameters within the ITPA SOL heat flux width database.

a/R_0	$\nu^{\rm omp}_{\rm gbs}$	$\rho^*_{\rm omp}$	$\beta_{\rm omp}$	κ	$I_{\rm p}$	$I_{\rm p}/A$	$P_{\rm tot}/V$	$P_{\rm tot}/S$	$P_{\rm tot}$	$B^{\rm omp}_{\rm pol}$	B_0	R_0	$\overline{n}_{\rm e}$	Corr. (%)
−17	−31	−18	**− 54**	−34	−36	−40	−23	−38	**− 51**	−49	27	−4	−15	q_{95}
	−18	32	40	49	27	36	18	11	19	40	−1	−25	35	a/R_0
		−39	13	38	36	13	−1	17	**51**	36	23	26	27	$\nu^{\rm omp}_{\rm gbs}$
			69	−22	**− 77**	36	**78**	**58**	**− 60**	−49	**− 83**	**− 92**	27	$\rho^*_{\rm omp}$
				35	−22	**54**	**72**	**70**	6	7	−49	**− 60**	48	$\beta_{\rm omp}$
					68	13	−13	2	**73**	**64**	26	32	15	κ
						6	−48	−24	**89**	**88**	**65**	**74**	4	$I_{\rm p}$
							79	**84**	21	**53**	21	**− 56**	**73**	$I_{\rm p}/A$
								95	−19	−3	−27	**− 88**	**62**	$P_{\rm tot}/V$
									11	20	−10	**− 68**	**65**	$P_{\rm tot}/S$
										86	**53**	**59**	18	$P_{\rm tot}$
											66	37	38	$B^{\rm omp}_{\rm pol}$
												47	22	B_0
													−45	R_0

Any parameter combination with too high mutual correlation (above ±50% marked in bold) should be excluded from scalings because the exponents in the scalings are too ambiguous.

Figure 5 presents a graphical overview of the 11 devices $\lambda_q^{\rm omp}$database, with the measured values plotted separately against each of the identified scaling parameters. The ITER parameter range is indicated in each case for the highest power operating point (7.5 MA) listed in table 2. The database clearly covers a wide range of parameters, but it is also evident that in many cases the range covered by any individual device is limited. This is a reflection of the fact that in many cases dedicated experiments were performed to obtain the heat flux profile data and were typically restricted in available machine time. This reduces the parameter range which can be covered. Moreover, in many devices, a large range is simply not accessible for limiter discharges. The exception is Tore Supra, whose points fill ~30% of the database, with strong variations of $\lambda_q^{\rm omp}$ on $I_{\rm p}$, input power and density. However, on Tore Supra these parameters are strongly correlated (within the database span the correlations among $I_{\rm p}$, P_Ω, q_{95}, $L_{\rm c}$ are all above 75%). Therefore, the influence of each alone on $\lambda_q^{\rm omp}$ is ambiguous and thus cannot be used for ITER prediction.

4. Scalings and recommendations for ITER

The scaling exercise has been performed in the standard way, seeking a mathematical expression $\lambda_q^{\rm omp} = f(p_1, p_2, \ldots, p_{15})$, with 15 parameters (see table 2 or 3). In order to include the poloidal angle dependence, transformation is made into the variable $(3 + \cos(\theta))$ which is always positive, vertically symmetric and for which the ratio LFS/HFS $= (3 + \cos(0))/(3 + \cos(\pi)) = 2$ is finite. Even with this transformation, however, the following regression finds no statistically significant dependence on the poloidal angle.

A power law form for the scaling is chosen because all of the parameters are positive definite and some span across more than a decade in the database. Since standard statistical toolboxes for multi-parameter fitting (using the weighted linear least-squares with robust standard errors as the criterion for best fit) are in the form of linear regression $y = \sum \alpha_i p_i$ instead of a power law $y = \prod_i p_i^{\alpha_i}$, the function $\lambda_q^{\rm omp} = f(p_1, p_2, \ldots, p_{15})$ must first be expressed in logarithmic polynomial form

$$\log\ \lambda_q^{\rm omp} = \sum_{i=0}^{15} \alpha_i \log\ p_i \qquad (3)$$

which corresponds to a power law. We then use the simple statistical toolbox *Gretl* [27] to look for scalings. A more appropriate technique would perhaps be the *principal component analysis* (using the *singular value decomposition* algorithm). However, it is unnecessarily complex and problematic in the case of our database with many missing values.

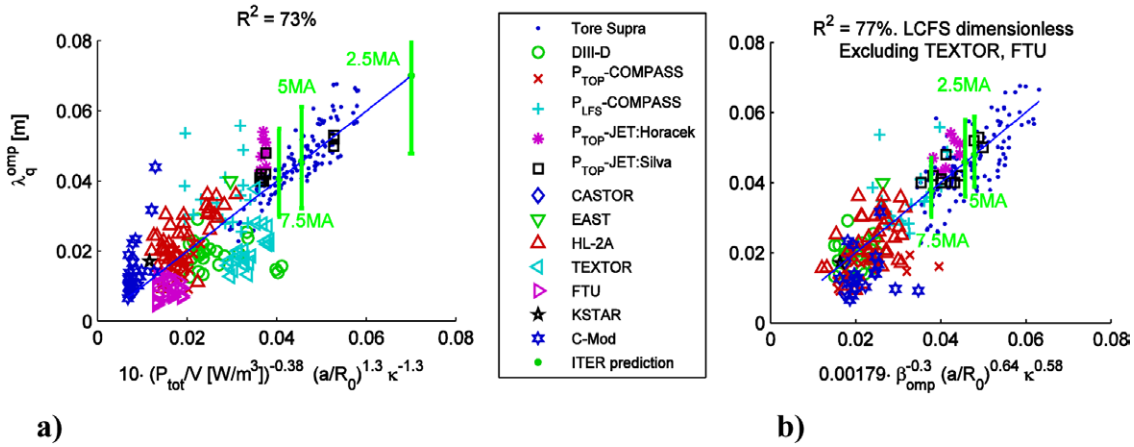

Figure 6. Two examples of scalings: (a) the most credible engineering scaling, depending on a/R_0, κ and P_{tot}/V; (b) the best dimensionless scaling (but note the highly uncertain measurement of midplane separatrix plasma pressure $\beta_{omp} = T_e^{LCFC} n_e^{LCFC} e/(2\mu_0 B_0^2)$). The corresponding ITER predictions are denoted by the green vertical bars representing 95% probability interval for the three ITER I_p-scenarios (see tables 2 and 4).

Using all available parameters within a single scaling yields a matrix close to singularity with extremely high exponents and no credible predictive capability. Instead, the following criteria are used to establish which groups of variables can be employed simultaneously in any given scaling:

- As shown in table 3, many of the parameters are mutually correlated in the database. For example, R_0 is correlated at -88% with P_{tot}/V. Thus, increasing freely the exponent on R_0 can be nearly fully compensated by increasing the exponent on P_{tot}/V and extrapolation to ITER would therefore be ambiguous. Similar comparisons can be drawn between other pairs of the chosen scaling variables. Within a single scaling only those parameters with low levels of mutual correlation should be used, excluding many parameter combinations.
- In statistical analysis, multiplication of two uncertain numbers (assuming zero mutual correlation) combines the relative errors, $\varepsilon =$ error/mean as

$$\epsilon\left(\prod_i p_i^{\alpha_i}\right) = \sqrt{\sum_i \alpha_i \epsilon_i^2}$$

  implying that the overall error is mostly determined by the most uncertain parameter and the fewer free parameters, the smaller the overall error. This suggests that the number of parameters within one scaling should be as small as possible, though errors on the main plasma parameters are usually unknown in the database and are assumed to be small (e.g. $\mathrm{err}(I_p)/I_p \ll 1$),
- Standard statistical theory suggests that those parameters for which the p-value of t-ratio $= p$(mean/standard deviation) $> 5\%$ [28] are *not statisticaly significant* and should therefore be excluded. Put another way, this means that the probability distribution of the exponent α_i spans significantly across zero. It is therefore highly probable that it can take also the value of zero and thus the respective parameter p_i should be excluded from the scaling since $p_i^0 = 1$.

Some further points are important in deciding which are the most appropriate subsets of the chosen parameters to use in the various scalings:

- parameters which explain most of the data variation (which we denote as *dominant*) are: β_{omp}, ρ^*_{omp}, $\frac{P_{tot}}{V}$, $\frac{P_{tot}}{S_{LCFS}}$, $\frac{P_{SOL}}{S_{LCFS}}$, I_p, P_{tot}, $\frac{I_p}{A}$ and B_{pol}^{omp}. These parameters are also strongly mutually correlated (see table 3). Therefore, only one of the nine dominant parameters can be used within any one scaling. All other parameters ($\overline{n}_e$, R_0, a/R_0, B_0, q_{95}, κ, θ) can be considered as *minor* modifications. On the other hand, a scaling without *any* dominant parameter yields too poor description of the data ($R^2 < 1/2$), and so is also excluded.
- Scalings with any exponent higher than 3 are excluded on the grounds of appearing unphysical.

The procedure in deriving scalings is as follows: begin with one chosen dominant parameters and add all other parameters, excluding combinations with high mutual correlations. A scaling constructed in this way have the highest possible descriptive capability (quantified by R^2), but most of the exponents would likely not be statistically significant. Subsequently removing those insignificant parameters (with many possible combinations in the order of removal) inevitably decreases R^2, though usually only very weakly.

This process yields less than a dozen suitable scalings. The two most credible ones are shown in figure 6, with the quality of each scaling again quantified by the index of determination, R^2. For each scaling, the ITER prediction λ_q^{ITER} is then calculated using the ITER values in table 2 with the error (vertical) bars given by the scaling data spread.

Finally, table 4 compiles λ_q^{ITER} predictions for the three characteristic values of I_p used in the ITER heat load specifications and the scalings found here are ordered by the statistical goodness of fit parameter, R^2.

5. Discussion of the scaling results

An uncertainty factor is present in the sense that the input data provided for the scaling exercise have been processed by individuals from each participating machine, an issue which complicates matters due to the different methods by which

Table 4. Overview of the most credible scalings (valid for tokamak inboard-limited plasmas) and consequent ITER predictions of the main SOL heat flux width at the outboard midplane for the three reference ITER plasma currents. Mapping to ITER inboard can be done simply by multiplying by the flux expansion of $\lambda_q^{\rm omp}/\lambda_q^{\rm imp} = 1.3$. The scalings are ordered by the overall fit quality quantified by the index of determination R^2. The presented error corresponds to the '95%-confidence interval' meaning that with 95% probability we predict for ITER e.g. for the 7.5 MA scenario, $44 - 11 < \lambda_q^{\rm omp}$ (mm) $< 44 + 11$. Scalings using $\beta_{\rm omp}$, $\rho^*_{\rm omp}$ or $\nu^{\rm omp}_{\rm gbs}$ are based on relatively imprecise (and in some cases unavailable, as in TEXTOR or FTU) omp probe measurements. These local plasma parameters are for ITER estimates only.

Scalings (dimensionless or in SI units)	$\lambda_q^{\rm omp}$ (mm) ITER prediction			Fit quality R^2
	2.5 MA	5.0 MA	7.5 MA	
$0.000\,34 \cdot q_{95}^{-0.25}(a/R_0)^{1.63}B_{\rm pol,omp}\ [\rm T]^{-0.65}\ \nu_{\rm gbs,omp}^{-0.1}\rho_{\rm omp}^{*-0.62}$	75 ± 14	57 ± 11	44 ± 9	83%
$3.61 \cdot (I_{\rm p}/A\ [\rm A\,m^{-2}])^{-0.41}(a/R_0)^{1.38}\kappa^{-1.32}\rho_{\rm omp}^{*-0.29}$	73 ± 17	48 ± 13	42 ± 10	78%
$0.001\,79 \cdot \beta_{\rm omp}^{-0.3}(a/R_0)^{0.64}\kappa^{0.58}$	49 ± 10	47 ± 11	39 ± 8	77%
$10 \cdot (P_{\rm tot}/V\ [\rm W\,m^{-3}])^{-0.38}(a/R_0/\kappa)^{1.3}$	67 ± 19	47 ± 15	42 ± 13	73%
$0.002\,19 \cdot q_{95}^{0.3}(a/R_0)^{0.6}\kappa^{-0.52}\nu_{\rm gbs,omp}^{-0.07}\rho_{\rm omp}^{*-0.32}$	72 ± 19	55 ± 17	46 ± 12	72%
$0.001 \cdot q_{95}^{0.35}\nu_{\rm gbs,omp}^{-0.088}\rho_{\rm omp}^{*-0.3}$	79 ± 18	63 ± 15	50 ± 12	70%
$53.5 \cdot q_{95}^{-0.16}B_0\ [\rm T]^{0.15}\ (a/R_0)^{0.93}\kappa^{-0.76}(P_{\rm tot}/S_{\rm LCFS}\ [\rm W\,m^{-2}])^{-0.46}$	57 ± 17	43 ± 14	38 ± 11	65%
$1.72 \cdot (P_{\rm tot}/V\ [\rm W\,m^{-3}])^{-0.28}q_{95}^{0.17}(a/R_0)^{0.96}$	88 ± 26	73 ± 21	56 ± 16	63%
$29.3 \cdot (a/R_0)^{0.67}(P_{\rm tot}/S_{\rm LCFS}\ [\rm W\,m^2])^{-0.45}$	64 ± 18	53 ± 15	41 ± 11	61%
Average	$\mathbf{69 \pm 18}$	$\mathbf{54 \pm 14}$	$\mathbf{44 \pm 11}$	

Langmuir probe characterstics are fitted and the varying probe techniques used. Most of the reasonable engineering scalings (e.g. figure 6(a)) slightly overestimate the experimental values from TEXTOR, DIII-D and FTU. In contrast, systematic underestimation is found for C-Mod, EAST, COMPASS (LFS measurement) and for some scalings also for JET. It is not possible to conclude that a specific 'human factor' leads to any systematic bias in the scalings, though a single individual (Horacek) did process the raw data from all COMPASS, TEXTOR and JET and this did not lead to any systematic shift with respect to the scalings. Nor does it appear that the particular technique used for the $T_{\rm e}$ measurement (e.g. BPP or standard single Langmuir probe) provides any correlation with a systematic departure of any group of data from a given scaling. The same JET discharges (80 831–80 838, 80 930–80 938, 81 003–81 015, 82 056–82 062) processed by both Horacek and Silva [29, 30] do not also yield significant systematic shift.

Fortunately, despite the uncertainties aluded to above, it appears that the majority of the scalings yield similar values when extrapolated to ITER at the three reference values of $I_{\rm p}$. This includes the scalings which make use of derived physics parameters, themselves dependent on the more uncertain midplane separatrix plasma parameters. Indeed, the top three best scalings in terms of R^2 parameter contain physics based variables. The best engineering scaling, with $R^2 = 73\%$, is $10 \cdot (P_{\rm tot}/V\ (\rm W\,m^{-3}))^{-0.38}(a/R_0/\kappa)^{1.3}$.

Given the similarity of the scaling predictions to ITER, table 4 also provides the average across all scalings of $\lambda_q^{\rm omp}$ for the ITER inner wall limiter reference plasma currents. The scalings are all consistent in predicting a decrease in the heat flux width with increasing $I_{\rm p}$, with $\lambda_q^{\rm omp} = 44 \pm 11$ mm for the most severe limiter heat exposure scenario of $I_{\rm p} = 7.5$ MA. Using the flux expansion factor of 1.3 from LFS to HFS, this 95% confidence interval becomes $\lambda_q^{\rm imp} = 57 \pm 14$ mm which is consistent with the ITER *inboard* FW panel shaping design value of 50 mm chosen for the broad main SOL heat flux width.

6. Conclusions

To hide misalignments between neighbouring plasma-facing panels on the ITER main chamber FW, the panels are toroidally shaped. This shaping increases the heat flux on the panel compared with an ideal cylindrical surface and this is a key disadvantage given the use of beryllium as armour material and the use of active cooling, which limit the steady state power handling capacity for limited plasmas which will characterize the start-up and ramp-down phases of all ITER plasmas. The shaping is thus optimized by careful choice of SOL parallel heat flux decay lengths. For the inboard midplane panels, it is now thought that two values of $\lambda_q^{\rm imp}$ are required to account for a narrow heat flux feature in the vicinity of the LCFS and a broader main SOL width. The latter was originally specified at $\lambda_q^{\rm imp} = 50$ mm for the design of the ITER toroidal shaping, based on a restricted (three tokamaks) experimental database of L-mode divertor plasma measurements.

This paper brings together and provides the statistical analysis of a significantly enlarged (eleven tokamaks) database, with dedicated measurements of λ_q extracted from Langmuir probe radial profiles of electron density and temperature obtained from inner wall limiter plasmas during experiments executed under the auspices of the ITPA, Divertor and SOL Topical Group. Multi-parameter regression analysis of data from ~400 probe reciprocations has yielded nine highly credible scalings using both engineering parameters and on theory-based [8] dimensionless plasma parameters. All of the scalings yield similar values for $\lambda_q^{\rm imp}$ when extrapolated to

the three ITER FW panel design reference plasma currents (2.5, 5.0 and 7.5 MA) and are consistent with the previous finding that the main SOL heat flux width decreases with increasing current. At the highest required power (I_p), the 95% confidence interval of the average value of inboard λ_q^{imp} across all the scalings is 43–71 mm, which is thus consistent with the ITER design choice of 50 mm.

Acknowledgments

This work was supported in part by the projects of Czech Science Foundation GA CR P205/12/2327, GA15-10723S and MSMT LM2011021, the US DOE under DE-FG02-07ER54917 and DE-AC02-09CH11466, DE-FC02-04ER54698. This work has been carried out within the Framework of the EUROfusion Consortium and has received funding from the Euratom research and training programme 2014–2018 under grant agreement number 633053 withing the European Union's Horizon 2020. The views and opinions expressed herein do not necessarily reflect those of the ITER Organization and of the European Commission. ITER is the Nuclear Facility INB-174. We acknowledge useful discussions with Renaud Dejarnac, Federico Halpern and Petr Dobias.

References

[1] Kocan M *et al* 2015 *Nucl. Fusion* **55** 033019
[2] Raffray A R 2014 *Nucl. Fusion* **54** 033004
[3] Mitteau R *et al* 2011 *J. Nucl. Mater.* **415** S969
[4] Stangeby P C and Mitteau R 2009 *J. Nucl. Mater.* **390–1** 963
[5] ITER Physics Expert Group on Divertor 1999 *Nucl. Fusion* **39** 2391
[6] Pitts R A *et al* 2011 *J. Nucl. Mater.* **415** S957
[7] Gunn J *et al* 2013 *J. Nucl. Mater.* **438** S184–S188
[8] Halpern F *et al Plasma Phys. Control. Fusion* submitted
[9] Stangeby P C 2000 *The Plasma Boundary of Magnetic Fusion Devices (Series in Plasma Physics and Fluid Dynamics)* (Abingdon: Taylor & Francis)
[10] LaBombard B *et al* 2007 *Rev. Sci. Instrum.* **78** 073501
[11] Boedo J A *et al* 1999 *Rev. Sci. Instrum.* **70** 2997
[12] Zhang W *et al* 2010 *Rev. Sci. Instrum.* **81** 113501
[13] Adamek J *et al* 2009 *J. Nucl. Mater.* **390** 1114–7
[14] Gunn J *et al* 2011 *Contrib. Plasma Phys.* **51** 256
[15] Horacek J *et al* 2010 *Nucl. Fusion* **50** 105001
[16] Stockel J 2007 *J. Phys.: Conf. Ser.* 012001
[17] Brotankova J 2009 *PhD Thesis* University of Charles, Prague
[18] Kocan M *et al* 2007 *J. Nucl. Mater.* **365** 1436
[19] Dejarnac R *et al* 2007 *Plasma Phys. Control. Fusion* **49** 1791
[20] Horacek J *et al* 2015 *J. Nucl. Mater.* **463** 385
[21] Adamek J *et al* 2011 *Proc. P1.059 of the EPS Conf. on Plasma Physics (France)* http://ocs.ciemat.es/EPS2011PAP/pdf/P1.059.pdf
[22] Garcia O E *et al* 2007 *Plasma Phys. Control. Fusion* **49** B47
[23] Pitts R A *et al* 2007 *J. Nucl. Mater.* **363–5** 505–10
[24] Gunn J P *et al* 2007 *J. Nucl. Mater.* **363–5** 484–90
[25] LaBombard B *et al* 2004 *Nucl. Fusion* **44** 1047–66
[26] Greenwald M 2002 *Plasma Phys. Control. Fusion* **44** R27
[27] http://gretl.sourceforge.net/
[28] https://en.wikipedia.org/wiki/P-value
[29] Silva C *et al* 2013 *J. Nucl. Mater.* **438** S189
[30] Silva C *et al* 2014 *Nucl. Fusion* **54** 083022
[31] Halpern F D *et al* 2013 *Nucl. Fusion* **53** 122001
[32] Romanelli F *et al* 2014 *Proc. of the 25th IAEA FEC (St. Petersburg, Russia)*